Decoherence in qubits due to low-frequency noise

New Journal of Physics
The open-access journal for physics

Decoherence in qubits due to low-frequency noise

J Bergli[1,5], Y M Galperin[1,2] and B L Altshuler[3,4]

[1] Department of Physics, University of Oslo, PO Box 1048, Blindern, 0316 Oslo, Norway
[2] A.F. Ioffe Physico-Technical Institute of Russian Academy of Sciences, 194021 St Petersburg, Russia
[3] Department of Physics, Columbia University, 538 West 120th Street, New York, NY 10027, USA
[4] NEC-Laboratories America, Inc., 4 Independence Way, Princeton, NJ 08540, USA
E-mail: jbergli@fys.uio.no

New Journal of Physics **11** (2009) 025002 (23pp)
Received 12 November 2008
Published 25 February 2009
Online at http://www.njp.org/
doi:10.1088/1367-2630/11/2/025002

Abstract. The efficiency of the future devices for quantum information processing will be limited mostly by the finite decoherence rates of the qubits. Recently, substantial progress was achieved in enhancing the time within which a solid-state qubit demonstrates coherent dynamics. This progress is based mostly on a successful isolation of the qubits from external decoherence sources. Under these conditions, the material-inherent sources of noise start to play a crucial role. In most cases, the noise that the quantum device demonstrates has a $1/f$ spectrum. This suggests that the environment that destroys the phase coherence of the qubit can be thought of as a system of two-state fluctuators, which experience random hops between their states. In this short review, the current state of the theory of the decoherence due to the qubit interaction with the fluctuators is discussed. The effect of such an environment on two different protocols of the qubit manipulations, free induction and echo signal, is described. It turns out that in many important cases the noise produced by the fluctuators is non-Gaussian. Consequently, the results of the interaction of the qubit with the fluctuators are not determined by the pair correlation function alone. We describe the effect of the fluctuators using the so-called spin-fluctuator model. Being quite realistic, this model allows one to exactly evaluate the qubit dynamics in the presence of one fluctuator. This solution is found, and its

[5] Author to whom any correspondence should be addressed.

features, including non-Gaussian effects, are analyzed in detail. We extend this consideration to systems of large numbers of fluctuators, which interact with the qubit and lead to the $1/f$ noise. We discuss existing experiments on the Josephson qubit manipulation and try to identify non-Gaussian behavior.

Contents

1. Introduction

Coherence in quantum solid-state devices inevitably suffers from fluctuations due to their environment. In particular, the rearrangement of electrons between traps in the insulating regions of the device, as well as stray flux tubes, causes pronounced fluctuations in many quantum devices. At low frequencies, a part of these fluctuations typically has a $1/f$ spectrum and is referred to as $1/f$ noise. Such noise is generic for all disordered materials (for a review, see e.g. [1, 2]); it is also common in single-electron and other tunneling devices, see e.g. [3]. Recent experiments [4, 5] on Josephson qubits indicated that charged impurities may also be responsible for noise. Low-frequency noise is specifically harmful since it is difficult to filter it out by finite band filters.

One of the most common sources of low-frequency noise is the rearrangement of dynamic two-state defects, *fluctuators*, see e.g. the book [6] and references therein. Random switching of a fluctuator between its two metastable states (1 and 2) produces random telegraph noise. The process is characterized by the switching rates γ_{12} and γ_{21} for the transitions $1 \to 2$ and $2 \to 1$. Only the fluctuators with energy splitting E less than temperature, T, contribute to the dephasing, since the fluctuators with large level splitting are frozen in their ground states (we measure temperature in energy units). As long as $E < T$ the rates γ_{12} and γ_{21} are close in magnitude, and without loss of generality one can assume that $\gamma_{12} \approx \gamma_{21} \equiv \gamma$, i.e. the fluctuations can be described as a *random telegraph process* (RTP), for reviews, see [6, 7]. A set of random

telegraph fluctuators with exponentially broad distribution of relaxation rates, γ, produces noise with a $1/f$ power spectrum at $\gamma_{\min} \ll \omega = 2\pi f \ll \gamma_0$. Here, $\gamma_{\min}$ is the switching rate of the 'slowest' fluctuator, whereas γ_0 is the maximal switching rate for the energy difference between the fluctuators' metastable states equal to temperature. Random telegraph noise has been observed in numerous nanodevices based on semiconductors, normal metals and superconductors [8].

Specific features observed in recent experiments [9] in Josephson phase qubits were interpreted in terms of resonant interaction of the qubit with two-level impurities. These experiments, as well as results [10] in a superconducting quantum circuit (quantronium), stimulated a very important attempt [11] to establish a relation between the contributions of two-level fluctuators with low and high frequencies. This has become possible because both the frequency domains contribute to the dephasing time and the energy relaxation time, respectively. However, this relation was significantly based on the assumption that the statistics of the fluctuations of the qubit parameters are Gaussian. In our view, this assumption is not obvious, and the main aim of this short review is to discuss the applicability range of the Gaussian approximation, as well as the deviations from the Gaussian approximation in connection with the problem of qubit dephasing. For this purpose, we will use a simple classical model within which one can evaluate exactly the qubit response to typical manipulation protocols. This model is often referred to as the *spin-fluctuator* (SF) model in similarity to the widely used and sometimes overused spin–boson model. According to the SF model, the quantum system—qubit—interacts with a set of two-level entities. The latter stochastically fluctuate between their states due to interaction with a thermal bath, which may not be directly coupled with the qubit. Since we are interested in the low-frequency noise generated by these switches, the latter can be considered as classical. Consequently, the system qubit + fluctuators can be described by relatively simple stochastic differential equations, which in many cases can be exactly solved. In particular, many results can just be borrowed from much earlier papers on magnetic resonance [12, 13], on spectral diffusion in glasses [14], as well as works on single-molecule spectroscopy [15].

The SF model has previously been used for the description of the effects of noise on various systems [16]–[21] and was recently applied to analysis of decoherence in charge qubits [22]–[30]. Various quantum and non-Markovian aspects of the model were addressed in [31]. These studies demonstrated, in particular, that the SF model is suitable for the study of non-Gaussian effects and that the latter may be essential in certain situations.

In this short review, we will address non-Gaussian effects in decoherence of Josephson qubits using the echo signal as an example. Resonant interaction between the qubit and fluctuators discussed in [9, 32, 33] will be left out. The paper is organized as follows. In section 2, we briefly describe decoherence in the Gaussian approximation. The SF model is described in section 3. Section 4 is aimed at a discussion of the relevance of the SF model to existing experiments, while current microscopic understanding of the two-level fluctuators is briefly reviewed in section 5.

2. Gaussian decoherence

A qubit is described by the generic Hamiltonian of a pseudospin $\frac{1}{2}$ in a 'magnetic field' $\mathbf{B}$, which can be time dependent:

$$\mathcal{H}_q = \tfrac{1}{2}\mathbf{B}\cdot\boldsymbol{\sigma}, \tag{1}$$

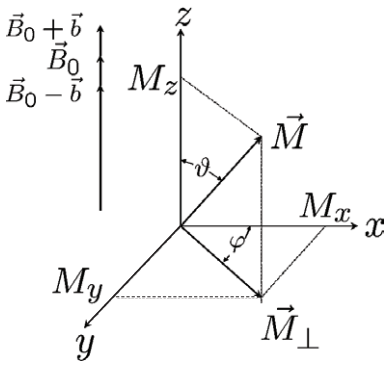

Figure 1. Bloch vector in the rotating frame of reference.

where σ_i are the Pauli matrices. It is well known that any state vector, $|\Psi\rangle$, of the qubit determines the Bloch vector $\mathbf{M}$ through the density matrix

$$\rho = |\Psi\rangle\langle\Psi| = \tfrac{1}{2}(\mathbf{1} + \mathbf{M}\cdot\boldsymbol{\sigma}). \tag{2}$$

The Schrödinger equation turns out to be equivalent to the precession equation for the Bloch vector:

$$\dot{\mathbf{M}} = \mathbf{B}\times\mathbf{M}. \tag{3}$$

The problem of decoherence arises when the 'magnetic field' is a sum of a controlled part $\mathbf{B}_0$ and a fluctuating part $\mathbf{b}(t)$, which represents the noise, i.e. is a stochastic process determined by its statistical properties, $\mathbf{B} = \mathbf{B}_0 + \mathbf{b}(t)$. The controlled part $\mathbf{B}_0$ is not purely static—to manipulate the qubit one has to apply certain high-frequency pulses of $\mathbf{B}_0$ in addition to the static fields applied between manipulation steps. In this paper, we will always assume that the manipulation pulses are short enough and neglect the decoherence during the pulses. Therefore, we need to consider only the effect of noise in the presence of static $\mathbf{B}_0$.

We will consider only the case where $\mathbf{b} \parallel \mathbf{B}_0$ and let the z-axis lie along the common direction of $\mathbf{B}_0$ and $\mathbf{b}$, see figure 1. This situation is called *pure dephasing* because the z-component of the Bloch vector, M_z, is conserved during the process. As long as the time evolution of $\mathbf{M}$ is governed by equation (3), the length $|\mathbf{M}|$ is also conserved, while the length $|\langle\mathbf{M}\rangle|$ of the vector $\mathbf{M}$ averaged over the stochastic process $\mathbf{b}$ decays. Description of this decay is the main objective of the decoherence theory. In the case of pure dephasing, this will be the decay of the components M_x and M_y. It is convenient to introduce a complex combination $m_+ = (M_x + \mathrm{i}M_y)/\sqrt{M_x^2 + M_y^2}$. Equation (3) can be written in terms of m_+ as

$$\dot{m}_+ = \mathrm{i}Bm_+ \quad \text{with solution} \quad m_+(t) = \mathrm{e}^{\int_0^t B(t')\,\mathrm{d}t'} m_+(0).$$

This solution has to be averaged over the stochastic process $\mathbf{b}(t)$. We define the phase $\phi(t)$ accumulated by m_+ as a sum of a regular, ϕ_0, and stochastic, φ, parts:

$$\phi(t) = \int_0^t \mathrm{d}t' B(t') = B_0 t + \int_0^t \mathrm{d}t' b(t') = \phi_0(t) + \varphi(t), \tag{4}$$

and obtain for average value of m_+

$$\langle m_+(t)\rangle = \langle \mathrm{e}^{\mathrm{i}\phi}\rangle m_+(0) = \mathrm{e}^{\mathrm{i}\phi_0}\langle \mathrm{e}^{\mathrm{i}\varphi}\rangle m_+(0).$$

The Gaussian approximation is based on the assumption that the probability distribution of the phase φ is Gaussian:

$$p(\varphi) = \frac{1}{\sqrt{2\pi\langle\varphi^2\rangle}} \mathrm{e}^{-\varphi^2/2\langle\varphi^2\rangle}. \tag{5}$$

As usual, this assumption is to be justified on the basis of the central limit theorem. The stochastic phase φ is the integral of the random process

$$v(t) \equiv b(t). \tag{6}$$

The Bloch vector precesses around the z-axis with the angular velocity that has random modulation $v(t)$. In the Gaussian approximation the only relevant statistical characteristic of $v(t)$ is the correlation function $\langle v(t_1)v(t_2)\rangle = W(|t_1 - t_2|)$ (we assume that $v(t)$ is a stationary random process). This function $W(\tau)$ vanishes at $\tau \to \infty$ and the scale of this decay is the correlation time, τ_c. If the time of integration, t, is much longer than τ_c the random phase $\varphi(t)$ is a sum of many uncorrelated contributions. The central limit theorem implies that such a sum has Gaussian distribution, independently of the details of the process. This is our initial understanding: the Gaussian approximation becomes valid as soon as t exceeds the correlation time of the noise. Below we will further discuss this conclusion. It follows from equation (5) that

$$\langle \mathrm{e}^{\mathrm{i}\varphi}\rangle = \int \mathrm{d}\varphi\, p(\varphi)\, \mathrm{e}^{\mathrm{i}\varphi} = \mathrm{e}^{-(1/2)\langle\varphi^2\rangle} \tag{7}$$

with

$$\langle\varphi^2\rangle = \int_0^t \mathrm{d}t_1 \int_0^t \mathrm{d}t_2\, \langle v(t_1)v(t_2)\rangle = \int_0^t \mathrm{d}t_1 \int_0^t \mathrm{d}t_2\, W(|t_1 - t_2|). \tag{8}$$

The correlator $W(\tau) = \langle v(t)v(t+\tau)\rangle$ is usually represented by its Fourier transform—the power spectrum of the noise, $S(\omega)$:

$$S(\omega) = \frac{1}{\pi} \int_0^\infty \mathrm{d}t\, W(t)\, \cos\,\omega t. \tag{9}$$

Using equations (4)–(9) we obtain

$$\langle\varphi^2\rangle = 4 \int_{-\infty}^{\infty} \mathrm{d}\omega\, \frac{\sin^2(\omega t/2)}{\omega^2}\, S(\omega). \tag{10}$$

For large t the identity

$$\lim_{a\to\infty} \frac{\sin^2 ax}{\pi a x^2} = \delta(x)$$

implies that $\langle\varphi^2\rangle \to 2\pi t\, S(0)$ and thus

$$\langle \mathrm{e}^{\mathrm{i}\varphi}\rangle = \mathrm{e}^{-t/T_2}, \qquad T_2^{-1} = \pi S(0). \tag{11}$$

Therefore, the Gaussian approximation leads to the exponential decay of the signal at large times, the decrement being given by the noise power at zero frequency.

2.1. Gaussian approximation: echo experiments

In the following, we will discuss the Bloch vector dynamics in the rotating frame of reference where $\phi_0 = 0$ and $m_+(t) = \mathrm{e}^{\mathrm{i}\varphi(t)}$. The time dependence of $\langle m_+\rangle = \langle \mathrm{e}^{\mathrm{i}\varphi}\rangle$ characterizes decay of

the so-called *free induction* signal [34]. In order to extract it in qubit experiments, one has to average over many repetitions of the same qubit operation. Even in setups that allow single-shot measurements [35] each repetition gives one of the two qubit states as the outcome. Only by averaging over many repeated runs can one see the decay of the average as described by the free induction signal. The problem with this is that the environment has time to change its state between the repetitions, and thus we average not only over the stochastic dynamics of the environment during the time evolution of the qubit, but over the initial states of the environment as well. As a result, the free induction signal decays even if the environment is too slow to rearrange during the operation time. This is an analogue of the inhomogeneous broadening of spectral lines in magnetic resonance experiments. This analogy also suggests ways to eliminate the suppression of the signal by the dispersion of the initial conditions. One can use the well-known echo technique (see e.g. [36]) when the system is subjected to a short manipulation pulse (the so-called π-pulse) with duration τ_1 at the time τ_{12}. The duration τ_1 of the pulse is chosen to be such that it switches the two states of the qubit. This is equivalent to reversing the direction of the Bloch vector and thus effectively reversing the time evolution after the pulse as compared with the initial one. As a result, the effect of any static field is canceled and decay of the echo signal is determined only by the *dynamics* of the environment. The decay of two-pulse echo can be expressed as $\langle m_+^{(e)}(2\tau_{12})\rangle$ [36], where

$$\langle m_+^{(e)}(t)\rangle \equiv \langle e^{i\psi(t)}\rangle, \qquad \psi(t) = \left(\int_0^{\tau_{12}} - \int_{\tau_{12}}^{t}\right) v(t')\,dt'. \tag{12}$$

Finite correlation time of $v(t)$ again leads to the Gaussian distribution of $\psi(t)$ at large enough t with

$$\langle \psi^2(2\tau_{12})\rangle = 16\int_{-\infty}^{\infty} d\omega \frac{\sin^4(\omega\tau_{12}/2)}{\omega^2} S(\omega). \tag{13}$$

This variance can be much smaller than $\langle\varphi^2\rangle$, equation (10), if $S(\omega)$ is singular at $\omega \to 0$.

3. Non-Gaussian decoherence: the SF model

We have discussed how to calculate the decoherence of a qubit in the Gaussian approximation. The only statistical characteristic of the noise is the time-correlation function, $W(t)$, or equivalently the power spectrum, $S(\omega)$. Now let us consider situations when this approximation is not valid. In such situations knowledge of only the noise power spectrum is not sufficient: noise sources with identical power spectra can have different decohering effects on the qubit. Thus, it is necessary to specify the model for the noise source in more detail. In the following, we will use a RTP as a model noise source. We will first analyze individual RTPs and show how $1/f$ noise appears as a result of averaging over a suitable ensemble of these processes. We will describe the decoherence due to one telegraph process, and finally extend this discussion to decoherence by averaging over ensembles of telegraph processes.

3.1. Random telegraph processes

Consider a stochastic function $\chi(t)$, which at any time takes the values $\chi(t) = \pm 1$ [7]. It is thus suitable for describing a system that can find itself in one of the two stable states, 1 and 2, and once in a while makes a switch between them. The switchings are assumed to be uncorrelated

random events with rates γ_{12} and γ_{21}, which in principle can be different. Here we will limit ourselves to the symmetric telegraph process: $\gamma_{12} = \gamma_{21} = \gamma$. The extension to the general case is straightforward, see e.g. [37]. The number k of switches that the fluctuator experiences within a time t follows a Poisson distribution

$$P_k = \frac{(\gamma t)^k}{k!} \mathrm{e}^{-\gamma t}. \tag{14}$$

The number of switches, k, determines the number of times the function $\chi(t)$ changes its sign contributing $(-1)^k$ to the correlation function, $C(t) \equiv \langle \chi(t)\chi(0)\rangle$. Therefore

$$C(t) = \mathrm{e}^{-\gamma t} \sum_{k=0}^{\infty} (-1)^k \frac{(\gamma t)^k}{k!} = \mathrm{e}^{-2\gamma t}, \quad t \geqslant 0. \tag{15}$$

The RTP results in fluctuating field $\mathbf{v}(t) = \mathbf{v}\chi(t)$ applied to the qubit. The magnitude of this field, $v = |\mathbf{v}|$, together with the switching rate, γ, characterizes the fluctuator. Using (9) we find the power spectrum of the noise generated by the ith fluctuator:

$$S_i(\omega) = v_i^2 \cdot \frac{1}{\pi} \frac{2\gamma_i}{(2\gamma_i)^2 + \omega^2}. \tag{16}$$

3.1.1. Generating $1/f$ noise by sets of telegraph processes. Let us consider a combination of a few statistically independent telegraph processes. Since the effective fields are all parallel to the z-axis we can characterize the ith fluctuator by a coupling strength v_i and a switching rate γ_i so that the total magnitude of the fluctuating field is given by $\sum_i v_i \chi_i(t)$. The total noise spectrum $S(\omega)$ equals a sum $\sum_i S_i(\omega)$. If the number of fluctuators interacting with the qubit is large, the fluctuating field can be written as a convolution of $S_i(\omega)$, equation (16), with the distribution $P(v, \gamma)$ of the parameters v and γ,

$$S(\omega) = \frac{1}{\pi} \int v^2 \, \mathrm{d}v \int \mathrm{d}\gamma \, \mathcal{P}(v, \gamma) \frac{2\gamma}{\omega^2 + (2\gamma)^2}. \tag{17}$$

To obtain the $1/\omega$ low-frequency behavior of the power spectrum (17), one has to assume that the distribution function $P(v, \gamma)$ behaves as $1/\gamma$ at small γ, i.e.

$$\mathcal{P}(v, \gamma)|_{\gamma \to 0} = \mathcal{P}(v)/\gamma. \tag{18}$$

In this case,

$$S(\omega) = \langle v^2 \rangle / \omega, \qquad \langle v^2 \rangle = \int_0^{\infty} v^2 \mathcal{P}(v) \, \mathrm{d}v. \tag{19}$$

It turns out that the distribution (18), which corresponds to a uniform distribution of $\log \gamma$, follows naturally from a simple model. In this commonly used model the role of a bistable fluctuator is played by a particle confined by a double-well potential [38]; each well has one state to host the particle, and the tunneling between these states is possible. This two-level system (TLS) describes a broad class of fluctuators: the particle can be a generalized particle moving in a generalized space. The Hamiltonian of a TLS with tunneling can be written as

$$\mathcal{H}_{\mathrm{F}} = \tfrac{1}{2} (\Delta \tau_z + \Lambda \tau_x), \tag{20}$$

where τ_i are the Pauli matrices (in contrast with the Pauli matrices σ_i that act in the qubit Hilbert space). Each TLS is characterized by two parameters—diagonal splitting, Δ, and the tunneling matrix element, $\Lambda = \hbar\omega_0 \, \mathrm{e}^{-\lambda}$. Here, ω_0 is a typical frequency of the classical motion of the

'particle' inside each of the two wells. The logarithm of the switching rate γ is proportional to the dimensionless tunneling integral λ. A natural assumption that λ is uniformly distributed in the TLS ensemble leads to the distribution (18) for the switching rate γ.

The environment is usually modeled as a thermal bath, which can represent a phonon field as well as e.g. electron–hole pairs in the conducting part of the system. Fluctuations in the environment affect the fluctuator through either Δ or Λ, equation (20). Assuming that the modulations of the diagonal splitting Δ are most important, we can describe the interaction of the environment with the qubit as

$$\mathcal{H}_{\mathrm{F-env}} = g'\hat{c}\tau_z, \tag{21}$$

where $\hat{c}$ is an operator in the Hilbert space of the environment depending on the concrete interaction mechanism. It is convenient to diagonalize $\mathcal{H}_{\mathrm{F}}$ (20) by rotating the fluctuator Hilbert space. Then

$$\mathcal{H}_{\mathrm{F}} = \frac{E}{2}\tau_z, \qquad E = \sqrt{\Delta^2 + \Lambda^2}.$$

Keeping the notation τ_i for the Pauli matrices representing the fluctuator in the rotated basis, we write the interaction Hamiltonian (21) as

$$\mathcal{H}_{\mathrm{F-env}} = g'\hat{c}\left(\frac{\Delta}{E}\tau_z - \frac{\Lambda}{E}\tau_x\right). \tag{22}$$

The factor $(\Lambda/E)^2$ appears in the inter-level transition rate [39, 40]:

$$\gamma(E, \Lambda) = (\Lambda/E)^2\,\gamma_0(E). \tag{23}$$

Here the quantity $\gamma_0(E)$ has the meaning of the *maximal* relaxation rate for fluctuators with a given energy splitting, E.

The parameters Δ and λ are usually supposed to be uniformly distributed over intervals much larger than those important for low-temperature kinetics [39, 41], so we can write their probability distribution as

$$\mathcal{P}(\lambda, \Delta) = P_0 \tag{24}$$

(leaving aside the problem of normalization, which will be fixed later). It is convenient to characterize each fluctuator by two parameters—the energy spacing between the levels, $E = \sqrt{\Delta^2 + \Lambda^2}$, and θ—determined through the relations $\Delta = E\cos\theta$, $\Lambda = E\sin\theta$ ($\theta \leqslant \pi/2$). The mutual distribution function of these parameters can be written as [42]

$$\mathcal{P}(E, \theta) = \frac{P_0}{\sin\theta}, \quad 0 \leqslant \theta \leqslant \frac{\pi}{2}. \tag{25}$$

Relaxation rates γ for the fluctuators with a given spacing E are distributed according to

$$\mathcal{P}(E, \gamma) = \frac{P_0}{2\gamma}\left[1 - \frac{\gamma}{\gamma_0(E)}\right]^{-1/2}, \quad \gamma_{\min}(E) \leqslant \gamma \leqslant \gamma_0(E). \tag{26}$$

To normalize this distribution one has to cut it off at small relaxation rates at a minimal value $\gamma_{\min}(E)$. The distribution (26) has equation (18) as its limit at $\gamma \ll \gamma_0$ and thus leads to $1/f$ noise in the frequency domain $\gamma_{\min} \ll \omega \ll \gamma_0$. The coupling, v, between the qubit and the fluctuator depends on the parameters E and θ of the fluctuator, see section 3.3 for more details. Since only the fluctuators with $E \lesssim T$ are important and both v and γ_0 are smooth functions of E, one can

use the values of v and γ_0 at $E = T$. Below we restrict ourselves by this approximation, which allows us to perform integration over the energy spacings of the fluctuator states. In particular, integrating equation (26) over E and γ, we connect P_0 with the total number, N_T, of thermally excited fluctuators:

$$P_0 = \frac{\mathcal{N}_T}{T\mathcal{L}}, \qquad \mathcal{L} \equiv \ln \frac{\gamma_0(T)}{\gamma_{\min}(T)}. \tag{27}$$

The integral expression (17) for the noise power spectrum is valid provided that $P_0 T \gg 1$, i.e. $\mathcal{N}_T \gg \mathcal{L}$. Substituting equation (27) into equation (17), we obtain the estimate

$$S(\omega) \sim \langle v^2 \rangle P_0 T \begin{cases} 1/\omega, & \gamma_{\min} \ll \omega \ll \gamma_0; \\ \gamma_0/\omega^2, & \omega \gg \gamma_0. \end{cases} \tag{28}$$

Therefore, the noise in the SF model indeed has the $1/f$ noise power spectrum at low enough frequencies. The crossover from ω^{-1} to ω^{-2} behavior at $\omega \sim \gamma_0$ manifests the cutoff in the distribution (26) at high switching rates.

3.2. Decoherence by a single RTP

3.2.1. Master equations. Having described the properties of random telegraph noise, we are now ready to discuss how it affects a qubit. Let us turn to equation (3) with a single telegraph process as the noise source.

We assume that the fluctuator does not feel any feedback from the qubit and thus the random telegraph function $\chi(t)$ equals $+1$ or -1 with the probability $\frac{1}{2}$ regardless of the direction of the Bloch vector $\mathbf{M}$. Consider the dynamics of the Bloch vector in the rotating frame of reference during a time interval $t, t+\tau$, which is small as compared with the inverse switching rate $1/\gamma$, so that the fluctuator changes its state with a small probability, $\gamma\tau \ll 1$, while the probability to switch more than once is negligible.

Let us split the probability of finding the angle φ at time t, $p(\varphi, t)$, into partial probabilities to arrive at the angle φ due to rotation around the vector $\mathbf{b}$ and $-\mathbf{b}$, respectively:

$$p(\varphi, t) = p_+(\varphi, t) + p_-(\varphi, t). \tag{29}$$

Denoting by $\mathcal{P}(\tau)$ the probability for a fluctuator *not* to switch during the time interval $(t, t+\tau)$ and by $\mathcal{Q}(\tau)$ the probability for it to switch once, one can express $p_+(\varphi, t+\tau)$ through $p_+(\varphi, t)$ and $p_-(\varphi, t)$:

$$p_+(\varphi, t+\tau) = \mathcal{P}(\tau) p_+(\varphi + v\tau, t) + \int_t^{t+\tau} \mathrm{d}t_1 \left\{ \dot{\mathcal{Q}}(t_1 - t) p_-[\varphi - v(t+\tau-t_1), t] \right\}. \tag{30}$$

A similar equation can be written for $p_-(\varphi, t+\tau)$:

$$p_-(\varphi, t+\tau) = \mathcal{P}(\tau) p_-(\varphi - v\tau, t) + \int_t^{t+\tau} \mathrm{d}t_1 \left\{ \dot{\mathcal{Q}}(t_1 - t) p_+[\varphi + v(t+\tau-t_1), t] \right\}. \tag{31}$$

When $\tau \ll \gamma^{-1}$ we can indeed neglect multiple switchings, and expand equation (14) as $\mathcal{P}(t) = P_0 = 1 - \gamma\tau$, $\mathcal{Q}(t) = P_1 = \gamma\tau$. Differentiating equations (30) and (31) over τ, we arrive at the set of equations:

$$\begin{aligned} \dot{p}_+ &= -\gamma p_+ + \gamma p_- + v\partial_\varphi p_+, \\ \dot{p}_- &= -\gamma p_- + \gamma p_+ - v\partial_\varphi p_-, \end{aligned} \tag{32}$$

$\partial_\varphi p_\pm \equiv \partial p_\pm/\partial\varphi$. Equations (32) can be combined into one second-order differential equation for $p(\varphi, t)$, equation (29),

$$\ddot{p} + 2\gamma\dot{p} = v^2\partial_\varphi^2 p\,, \tag{33}$$

which is known as the telegraph equation. We can always choose the x-direction in such a way that $\varphi = 0$ at $t = 0$. Thus $p(\varphi, 0) = \delta(\varphi)$. The second initial condition to equation (33), $\dot{p}(\varphi, 0) = \pm 2v\partial_\varphi p(\varphi, 0)$, follows directly from the integral equation (30). The sign depends on the initial state of the fluctuator. After averaging over the fluctuator's initial state, $\dot{p}(\varphi, 0) = 0$.

To evaluate the decoherence for this model we multiply equation (33) by $m_+ = \mathrm{e}^{\mathrm{i}\varphi}$ and integrate over φ to show that the mean value of m_+,

$$\langle m_+\rangle = \langle \mathrm{e}^{\mathrm{i}\varphi}\rangle = \int \mathrm{d}\varphi\, p(\varphi)\, \mathrm{e}^{\mathrm{i}\varphi},$$

satisfies the equation

$$\langle \ddot{m}_+\rangle + 2\gamma\langle \dot{m}_+\rangle = -v^2\langle m_+\rangle. \tag{34}$$

The initial condition for this equation is $m_+(0) = 1$ since $\varphi(0) = 0$. The second initial condition, $\dot{m}_+(0) = 0$, follows from the boundary condition $\dot{p}(\phi, 0) = 0$. The solution of equation (34) with these initial conditions,

$$\langle m_+\rangle = \frac{\mathrm{e}^{-\gamma t}}{2\mu}\left[(\mu+1)\mathrm{e}^{\gamma\mu t} + (\mu-1)\mathrm{e}^{-\gamma\mu t}\right], \quad \mu \equiv \sqrt{1 - \frac{v^2}{\gamma^2}}\,, \tag{35}$$

describes decoherence of a qubit due to a single RTP given by the coupling strength v and the switching rate γ.

According to (35), the free induction signal demonstrates qualitatively different behaviors for large and small ratios v/γ. At $v \gg \gamma$ one can consider the qubit as a quantum system experiencing beatings between the states with different splittings, $\mathbf{B}_0 \pm \mathbf{b}$, the width of these states being γ. In the opposite limiting case, $v \ll \gamma$, the inter-level splitting is self-averaged to a certain value, the width being $v^2/2\gamma$. This situation was extensively discussed in connection with the magnetic resonance and is known as the *motional narrowing of spectral lines* [12]. The two types of behavior will be discussed in more detail in section 4.

3.2.2. Comparison with the Gaussian approximation. Let us now compare equation (35) with the result (11) of the Gaussian approximation. Substituting (16) for the noise power spectrum, one obtains

$$\frac{1}{T_2^{(\mathrm{G})}} = \frac{v^2}{2\gamma}\,. \tag{36}$$

When discussing the Gaussian approximation we argued that it should be valid for times longer than the correlation time of the noise, which for the RTPs is $(2\gamma)^{-1}$. Expanding our equation (35) at long times we find that it indeed decays exponentially (or the oscillations decay exponentially in the case $v > \gamma$). However, the rate of the decay is parametrically different from equation (36):

$$\frac{1}{T_2} = \gamma - \gamma\,\mathrm{Re}\sqrt{1 - \frac{v^2}{\gamma^2}}\,. \tag{37}$$

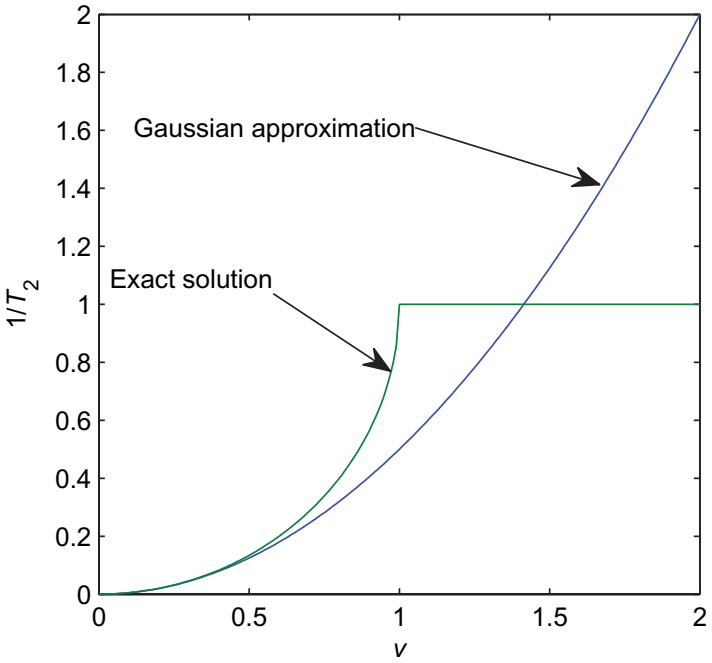

Figure 2. Comparison of the decoherence rate T_2^{-1} for a single random telegraph process and the corresponding Gaussian approximation.

It is easy to check that in the limit $v \ll \gamma$, equation (37) coincides with the Gaussian result. Shown in figure 2 are equations (36) and (37) as functions of v for fixed $\gamma = 1$. We see that the Gaussian approximation is only valid in the limit $v \ll \gamma$. Apparently, this conclusion is in contradiction to the previous discussion based on the central limit theorem. It looked convincing that according to this theorem $p(\varphi, t)$ *always* tends to a Gaussian distribution with time-dependent variance provided that the time exceeds the correlation time of the noise.

To resolve this apparent contradiction, let us analyze the shape of the distribution function, $p(\varphi, t)$, which follows from equation (33). The solution of this equation with the boundary conditions $p(\varphi, 0) = \delta(\varphi)$ and $\dot{p}(\varphi, 0) = 0$ is [30]:[6]

$$p(\varphi,t) = \frac{1}{2}\mathrm{e}^{-\gamma t}\left[\delta(\varphi+vt)+\delta(\varphi-vt)\right] + \frac{\gamma}{2v}\mathrm{e}^{-\gamma t}\left[\Theta(\varphi+vt)-\Theta(\varphi-vt)\right] \times \left[\frac{I_1\left(\gamma t\sqrt{1-(\varphi/vt)^2}\right)}{\sqrt{1-(\varphi/vt)^2}} + I_0\left(\gamma t\sqrt{1-(\varphi/vt)^2}\right)\right], \tag{38}$$

where $I_v(x)$ is the modified Bessel function and $\Theta(x)$ is the Heaviside step function:

$$\Theta(x) = \begin{cases} 1, & x > 0\,, \\ 0, & x < 0\,. \end{cases}$$

The distribution function (38) (shown in figure 3 for various t values) consists of two delta functions and a central peak.

[6] Note that in [30] the term with I_0 was missing.

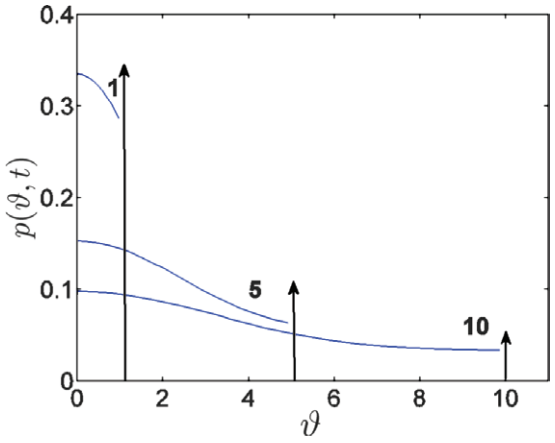

Figure 3. The distribution function (38) for $t = 1$, 5 and 10 (only the part for positive φ is shown; the function is symmetric). $v = \gamma = 1$. The arrows represent the delta functions (not to scale).

The delta functions represent the finite probability for the fluctuator to be in the same state during time t. As time increases, the weight of the delta functions decreases and the central peak broadens. At long times, this peak acquires a Gaussian shape. Indeed, at $\gamma t \gg 1$ one can use the asymptotic behavior of the Bessel function $I_v(z) \to (2\pi)^{-1/2} e^z$, as $z \to \infty$. For $\varphi \ll vt$ we can also expand $\sqrt{1-(\varphi/vt)^2}$ and convince ourselves that the central peak in accordance with the central limit theorem is indeed described by the Gaussian distribution (5) with the variance $\langle \varphi^2 \rangle = v^2 t/\gamma$. If the qubit–fluctuator coupling is weak, $v \ll \gamma$, this Gaussian part of $p(\varphi, t)$ dominates the average $\langle e^{i\varphi} \rangle$ and the Gaussian approximation is valid. Contrarily, for the strong coupling, $v > \gamma$, the average is dominated by the delta functions at the ends of the distribution, and the decoherence demonstrates a pronounced non-Gaussian behavior, even at $t > \gamma^{-1}$.

Unfortunately, it is impossible to measure the distribution of φ experimentally. Indeed, each experimental shot corresponds to a particular realization of the random external noise and does not yield a particular value of φ. The reason lies in the difference between the qubit that can be viewed as a pseudospin $\frac{1}{2}$ and a classical Bloch vector $\mathbf{M}$. According to equation (2), the components M_x, M_y, M_z of $\mathbf{M}$ are connected with the mean component of the final state of the pseudospin. Therefore, to measure the value of the phase φ (argument of m_+) that corresponds to a given realization of the noise, one would have to repeat the experimental shot with *the same realization of the noise* many times. This is impossible, because each time the realization of noise is different. Therefore, the only observable in the decoherence experiments is the average $\langle e^{i\varphi} \rangle$. There is no way to extract more information about the distribution $p(\varphi, t)$ from any experiment with a single qubit.

3.3. Averaging over ensembles of RTPs

3.3.1. General expressions. As we have seen, a set of fluctuators characterized by the distribution function (26) of relaxation rates provides a realistic model for $1/f$ noise. Thus, in order to study the decoherence by such a noise, it is natural to sum contributions of many fluctuators. To perform this procedure we assume that the dynamics of different fluctuators are not correlated, i.e. $\langle \chi_i(t)\chi_j(t') \rangle = \delta_{ij} e^{-2\gamma_i |t-t'|}$. Under this assumption, the average value of the

complex momentum, $\langle m_+\rangle$, is just a product of the partial averages,

$$\langle m_+(t)\rangle = \prod_i \langle m_{+i}(t)\rangle = \mathrm{e}^{\sum_i \ln\langle m_{+i}(t)\rangle}.$$

Since the logarithm of a product is a self-averaging quantity, it is natural to approximate the sum of logarithms, $\sum_i \ln\langle m_+(t)\rangle_i$, by its average value, $-\mathcal{K}_m(t)$, where

$$\mathcal{K}_m(t) \equiv -\overline{\sum_i \ln\langle m_{+i}(t)\rangle}\,. \tag{39}$$

Here, the bar denotes the average over both the coupling constants, v, of the fluctuators and their transition rates, γ. If the number $\mathcal{N}_\mathrm{T}$ of thermally excited fluctuators is large we can replace the sum $\sum_i \ln\langle m_{+i}\rangle$ by $\mathcal{N}_\mathrm{T}\,\overline{\ln\langle m_+\rangle}$. Furthermore, one can employ the Holtsmark procedure [43], i.e. to replace $\overline{\ln\langle m_+\rangle}$ by $\overline{\langle m_+\rangle - 1}$, assuming that each of $\langle m_{+i}\rangle$ is close to 1. Thus, $\mathcal{K}_m(t)$ is approximately equal to

$$\mathcal{K}_m(t) \approx \mathcal{N}_\mathrm{T}\overline{(1-\langle m_+\rangle)} = \int \mathrm{d}v\,\mathrm{d}\gamma\,\mathcal{P}(v,\gamma)\left[1-\langle m_+(v,\gamma|t)\rangle\right]. \tag{40}$$

Here $\langle m_+(v,\gamma|t)\rangle$ depends on the parameters v and γ according to equation (35). The average free induction signal is then $\overline{\langle m_+(t)\rangle} = \mathrm{e}^{-\mathcal{K}_m(t)}$.

Analysis of the echo signal is rather similar: one has to replace $\langle m_+(t)\rangle$ taken from equation (35) by [42]

$$\langle m_+^{(\mathrm{e})}(2\tau_{12})\rangle = \frac{\mathrm{e}^{-2\gamma\tau_{12}}}{2\mu^2}\left[(\mu+1)\,\mathrm{e}^{2\gamma\mu\tau_{12}} - (\mu-1)\,\mathrm{e}^{-2\gamma\mu\tau_{12}} - \frac{2v^2}{\gamma^2}\right]. \tag{41}$$

To evaluate the time dependence of either the free induction or the echo signal, one has to specify the distribution of the coupling constants v. Let us consider each fluctuator as a two-level tunneling system characterized by the Hamiltonian

$$\mathcal{H}_F^{(i)} = \tfrac{1}{2}\left(\Delta_i\tau_z^{(i)} + \Lambda_i\tau_x^{(i)}\right), \tag{42}$$

where $\tau^{(i)}$ is the set of Pauli matrices describing the ith two-state fluctuator. The energy splitting for each fluctuator is $E_i = \sqrt{\Delta_i^2+\Lambda_i^2}$. The variation of the energy spacing between the states of the qubit can be cast into the effective Hamiltonian, which (after a rotation similar to that in equation (22)) acquires the form

$$\mathcal{H}_{q\mathrm{F}} = \sum_i v_i\,\sigma_z\tau_z^{(i)}, \qquad v_i = g(r_i)\,A(\mathbf{n}_i)\cos\theta_i. \tag{43}$$

Here $\theta_i \equiv \arctan(\Lambda_i/\Delta_i)$, $\mathbf{n}_i$ is the direction of elastic or electric dipole moment of the ith fluctuator, and r_i is the distance between the qubit and the ith fluctuator. Note that in equation (43) we neglected the term proportional to $\sigma_z\tau_x$. This can be justified as long as the fluctuator is considered to be a classical system. The functions $A(\mathbf{n}_i)$ and $g(r_i)$ are not universal.

The coupling constants, v_i, determined by equation (43), contain $\cos\theta_i$ and thus are statistically correlated with θ_i. It is convenient to introduce an uncorrelated random coupling parameter, u_i, as

$$u_i = g(r_i)A(\mathbf{n}_i), \qquad v_i = u_i\,\cos\theta_i. \tag{44}$$

It is safe to assume that the direction, $\mathbf{n}_i$, of a fluctuator is correlated neither with its distance from the qubit, r_i, nor with the tunneling parameter represented by the variable θ_i. This assumption allows us to replace $A(\mathbf{n})$ by its average angle, $\bar{A} \equiv \langle A(|\mathbf{n})|\rangle_\mathbf{n}$.

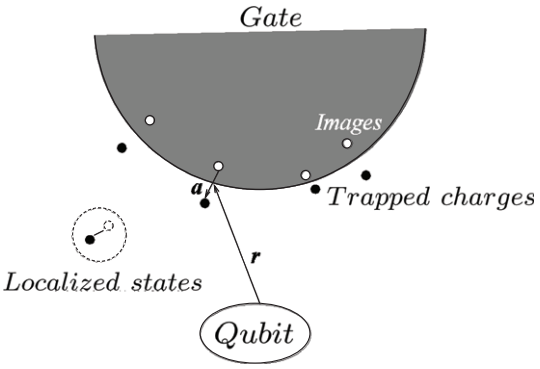

Figure 4. Sketch of localized charges near an electrode. Induced image charges create local dipoles that interact with the qubit.

3.3.2. Simple model. The coupling parameter, g, decays with distance, r, between the qubit and the fluctuator. Usually this decay is algebraic: $g(r) \propto \bar{g}/r^b$. We will distinguish between two cases: (i) the fluctuators are distributed in three-dimensional space ($d = 3$) and (ii) the fluctuators are located in the vicinity of a two-dimensional manifold, e.g. in the vicinity of the interface between an insulator and a metal ($d = 2$). Using the distribution (26) of the relaxation rates one can express $\mathcal{P}(u, \theta)$ as

$$\mathcal{P}(u,\theta) = (\eta \cos\theta)^{d/b} \frac{1}{\sin\theta} \frac{1}{u^{(d/b)+1}}, \quad \eta \equiv \frac{\bar{g}}{r_{\mathrm{T}}^b}, \qquad r_{\mathrm{T}} \equiv \frac{a_d}{(P_0 T)^{1/d}}. \tag{45}$$

Here a_d is a d-dependent dimensionless constant, whereas r_{T} is a typical distance between the fluctuators with $E_i \lesssim T$. In the following we will, for simplicity, assume that

$$r_{\min} \ll r_T \ll r_{\max}, \tag{46}$$

where $r_{\min}$ ($r_{\max}$) are distances between the qubit and the closest (most remote) fluctuator. Under this condition $\eta \propto T^{b/d}$ is the typical constant of the qubit–fluctuator coupling. As soon as the inequality (46) is violated the decoherence starts to depend explicitly on either $r_{\min}$ or $r_{\max}$, i.e. becomes sensitive to particular mesoscopic details of the device.

Let us first consider the case when $d = b$, as it is for charged traps located near the gate electrode (where $b = d = 2$ due to the dipole nature of the field produced by a charge and its induced image, see figure 4). In this case, one can cast equation (40) into the form

$$\mathcal{K}_f(t) = \eta \int \frac{\mathrm{d}u}{u^2} \int_0^{\pi/2} \mathrm{d}\theta \tan\theta \left[1 - f(u\cos\theta, \gamma_0 \sin^2\theta | t)\right]. \tag{47}$$

Here $f(v, \gamma|t)$ is equal either to $\langle m_+(v,\gamma|t)\rangle$ or to $\langle m_+^{(\mathrm{e})}(v,\gamma|t)\rangle$, depending on the manipulation protocol. Equation (47) together with equations (35) and (41) allows one to analyze different limiting cases.

In the case of two-pulse echo it is instructive to look at the asymptotic behaviors of $\mathcal{K}_f(t)$. From equation (41) it follows that

$$1 - \langle m_+^{(\mathrm{e})}(u\cos\theta, \gamma_0 \sin^2\theta|t)\rangle \propto \begin{cases} t^3\gamma_0 \sin\theta (u\cos\theta)^2, & t \ll (\gamma_0 \sin\theta)^{-1}, \\ t^2 (u\cos\theta)^2, & (\gamma_0\sin\theta)^{-1} \ll t \ll u^{-1}, \\ tu\cos\theta, & u^{-1} \ll t. \end{cases} \tag{48}$$

Splitting the regions of integration over u and θ according to the domains (48) of different asymptotic behaviors, one obtains

$$\mathcal{K}_m(2\tau_{12}) \sim \eta\tau_{12}\min\{\gamma_0\tau_{12}, 1\}\,. \tag{49}$$

The dephasing time (defined for non-exponential decay as the time when $\mathcal{K} \sim 1$) for the two-pulse echo decay is thus equal to

$$\tau_\varphi = \max\left\{\eta^{-1}, (\eta\gamma_0)^{-1/2}\right\}. \tag{50}$$

The result for $\gamma_0\tau_{12} \ll 1$ has a clear physical meaning [42]: the decoherence occurs only provided that at least one of the fluctuators flips. Each flip provides a contribution $\sim \eta t$ to the phase, while $\gamma_0\tau_{12} \ll 1$ is a probability for a flip during the observation time. The result for $\gamma_0\tau_{12} \gg 1$ is less intuitive since in this region the dephasing is non-Markovian, see [42] for more details.

It is important that at long observation times, $\tau_{12} \gg \gamma_0^{-1}$, the decoherence is dominated by few *optimal* fluctuators. The distance, $r_{\rm opt}(T)$, between the optimal fluctuators and the qubit is determined by the condition

$$v(r_{\rm opt}) \approx \gamma_0(T)\,. \tag{51}$$

Derivation of equation (51) requires a rather tedious analysis of the expansion (48) and the integration over u and θ, see [25, 42] for more details. This estimate emerges naturally from the behavior of the decoherence in the limiting cases $v \gg \gamma$ and $v \ll \gamma$. For strong coupling, the fluctuators are slow and the qubit's behavior is determined by quantum beatings between the states with $E \pm v$. Accordingly, the decoherence rate is of the order of γ. In the opposite case, as we have already discussed, the decoherence rate is $\propto v^2/\gamma$. Matching these two limiting cases one arrives at the estimate (51).

What if $d \neq b$? If the coupling decays as $1/r^b$ and the fluctuators are distributed in a d-dimensional space, then $r^{d-1}\,{\rm d}r \to \mathcal{P}(v) \propto v^{-(1+(d/b))}$. As a result, at $d \leqslant b$ the decoherence is controlled by optimal fluctuators located at the distance $r_{\rm opt}$ *provided that they exist*. At $d > b$ the decoherence at large time is determined by most remote fluctuators with $v = v_{\rm min}$. If $d \leqslant b$, but the closest fluctuator has $v_{\rm max} \ll \gamma_0$, then it is the quantity $v_{\rm max}$ that determines the decoherence. In the last two cases, $\mathcal{K}(t)$ is proportional to t^2, and one can apply the results of [22], substituting for v either $v_{\rm min}$ or $v_{\rm max}$.

Since $r_{\rm opt}$ depends on the temperature, one can expect crossovers between different regimes as a function of temperature. A similar mesoscopic behavior of the decoherence rate was discussed for a microwave-irradiated Andreev interferometer [44].

Note that the result (49) for the long-range interaction cannot be reproduced by the Gaussian approximation since in the latter case the decoherence would be determined by the nearest neighbors of the qubit. That can be seen from explicit expression for the phase accumulation following from the Gaussian model, see equation (52) below. Being substituted into equation (47) this expression leads to divergence of the integral over u at its upper limit, which physically means the dominating role of nearest neighbors of the qubit. At the same time, the SF model implies that the most important contributions are given by the fluctuators with $v(r) \sim \gamma_0$.

The above procedure still leaves unanswered a delicate question: can contributions of several fluctuators be described by averages over the fluctuators' parameters? The situation with a qubit interacting with environment in fact differs from that of a resonant TLS in spin or phonon echo experiments. In the first case the experiment is conducted using a single qubit

surrounded by a set of fluctuators with fixed locations, while in the second case *many* resonant TLSs participate in the absorption. Consequently, one can assume that each TLS has its own environment and calculate the properties averaged over positions and transition rates of the surrounding fluctuators. How many surrounding fluctuators does one need to replace the set of fluctuators with fixed locations (and transition rates) by an averaged fluctuating medium? This issue was studied numerically in [25]. The analysis showed that one really needs many ($\gtrsim$100) fluctuators to avoid strong mesoscopic fluctuations.

4. Relevance to experiments

In this section, we will briefly review some experiments where we believe that the theory of non-Gaussian noise is relevant. While there are some indications of non-Gaussian behavior, to our knowledge, the existing experiments are not conclusive enough. However, we should emphasize that observation of non-Gaussian effects was not among the goals of these experiments. The main goal was to achieve the longest possible decoherence times. Probably, as progress is made, the situations where only one or a few independent noise sources are important would become usual rather than exceptional, making the non-Gaussian effects more pronounced. We also believe that experimental studies of the non-Gaussian effects would provide useful information on the environmental degrees of freedom. Therefore devices showing pronounced non-Gaussian behavior, while not necessarily being the optimal qubits, may serve as useful research tools.

4.1. Plateaus in the echo signal

Using equations (11) and (36) we have calculated the decay of the free induction signal due to a single fluctuator in the Gaussian approximation at long times. Let us return to equation (13) and evaluate the same for the echo signal, but at arbitrary times. The result is

$$\langle \psi^2 \rangle = \frac{v^2}{2\gamma^2}\left[4\gamma\tau_{12} - 3 + 4\mathrm{e}^{-2\gamma\tau_{12}} - \mathrm{e}^{-4\gamma\tau_{12}}\right] \tag{52}$$

with $\langle m_+^{(\mathrm{e})} \rangle = \mathrm{e}^{-\langle\psi^2\rangle/2}$ as before. This should be compared with the exact result, equation (41). In figure 5 both results are shown for both a weakly ($v/\gamma = 0.8$) and a strongly ($v/\gamma = 10$) coupled fluctuator. As has been discussed before, the Gaussian approximation is accurate for $v \lesssim \gamma$, while at $v > \gamma$ the two results are qualitatively different. In particular, the plateaus in the time dependence of the echo signal shown in figure 5 are beyond the Gaussian approximation. We believe that such a plateau was experimentally observed in [45] (see figure 3 in [45]). In the limit $v \gg \gamma, \sqrt{\gamma/\tau}$, equation (41) acquires a simple form:

$$\langle m_+^{(\mathrm{e})} \rangle = \mathrm{e}^{-2\gamma\tau}\left[1 + \frac{\gamma}{v}\sin 2v\tau\right]. \tag{53}$$

According to equation (53), the plateau-like features ($\mathrm{d}\langle m_+^{(\mathrm{e})}\rangle/\mathrm{d}\tau \approx 0$) occur at $v\tau \approx k\pi$ and their heights $\langle m_+^{(\mathrm{e})}\rangle \approx \mathrm{e}^{-2\pi k\gamma/v}$ exponentially decay with the number k. Measuring experimentally the position and the height of the first plateau, one can determine both the fluctuator coupling strength v and its switching rate γ. For example, the echo signal measured in [45] shows a plateau-like feature at $\tau_{12} = 3.5$ ns at the height $\langle m_+^{(\mathrm{e})}\rangle = 0.3$, which yields $v \approx 143$ MHz and $\gamma \approx 27$ MHz. If the fluctuator is a charge trap near the gates producing a dipole electric field, its coupling strength is $v = \mathrm{e}^2(\mathbf{a}\cdot\mathbf{r})/r^3$. Using the gate–qubit distance

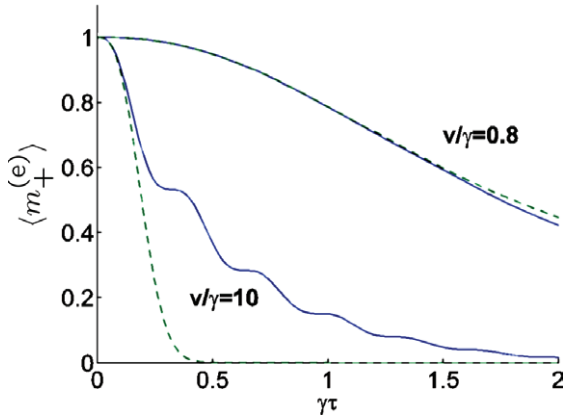

Figure 5. Echo signal for different values of the ratio v/γ (shown near the curves), equation (41). Dashed lines—calculations along the Gaussian approximation, equation (52).

$r \approx 0.5\,\mu$m, we obtain a reasonable estimate for the tunneling distance between the charge trap and the gate, $a \sim 20$ Å. A more extensive discussion of this is found in [28].

4.2. Flux qubit

In section 3.3 we discussed a model with a broad distribution of coupling strengths, v. This is appropriate in a situation where the noise sources are distributed uniformly in space and act on the qubit via a long-range (power law) force. In this section, we wish to apply the SF model to experiments on flux qubits [46, 47]. Since the microscopic source of flux noise is not clarified (see e.g. [48] and references therein), it is not clear what would be the most reasonable distribution of v. We have adopted the simplest model, where the coupling parameters v are narrowly distributed around some characteristic value $\bar{v}$. In other words, v and γ are supposed to be uncorrelated, $\mathcal{P}(v,\gamma) = \mathcal{P}_v(v)\mathcal{P}_\gamma(\gamma)$, and

$$\mathcal{P}_\gamma(\gamma) = \frac{P_0 T}{\gamma}\Theta(\gamma_0 - \gamma)\Theta(\gamma - \gamma_{\min}), \qquad \mathcal{P}_v(v) = \delta(v - \bar{v}). \tag{54}$$

Using equation (54) and the expressions for $\langle m_+^{(e)}\rangle$ for either the Gaussian (equation (52)) or the SF (equation (41)) models, we obtain the quantity $\mathcal{K}$ defined in equation (39). In the Gaussian model:

$$\mathcal{K}_G(2\tau_{12}) = 2P_0 T\bar{v}^2\tau_{12}^2 \times \begin{cases} 2\gamma_0\tau_{12}/3, & \gamma_0\tau_{12} \ll 1, \\ \ln 2, & \gamma_0\tau_{12} \gg 1. \end{cases} \tag{55}$$

We see that at long times, $\gamma_0\tau_{12} \gg 1$, we have a quadratic dependence on time, which manifests a Gaussian decay of the echo signal. At short times, $\gamma_0\tau_{12} \ll 1$, the result is multiplied by an additional factor $\gamma_0\tau$, which is the probability for a single flip of the fastest fluctuators.

In the SF model there are two limiting cases.

(i) When $\bar{v} \ll \gamma_0$

$$\mathcal{K}_{sf}(2\tau_{12}) \approx \begin{cases} 4P_0 T\gamma_0\bar{v}^2\tau_{12}^3/3, & \tau_{12} \ll \gamma_0^{-1}, \\ P_0 T(2\ln 2)\bar{v}^2\tau_{12}^2, & \gamma_0^{-1} \ll \tau_{12} \ll \bar{v}^{-1}, \\ P_0 T\alpha\bar{v}\tau_{12}, & \bar{v}^{-1} \ll \tau_{12}, \end{cases} \tag{56}$$

where $\alpha \approx 3$. At small times $\tau_{12} \ll \bar{v}$ we arrive at the same result as in the Gaussian approach, equation (55). However, at large times, $\tau_{12} \gg \bar{v}^{-1}$, the exact result dramatically differs from the prediction of the Gaussian approximation. To understand the origin of the non-Gaussian behavior notice that for $\mathcal{P}_\gamma(\gamma) \propto 1/\gamma$, the decoherence is dominated by the fluctuators with $\gamma \approx v$. Indeed, very 'slow' fluctuators produce slow varying fields, which are effectively refocused in the course of the echo experiment. As to the 'too fast' fluctuators, their influence is reduced due to the effect of motional narrowing. We have already learned that only the fluctuators with $v \ll \gamma$ produce Gaussian noise. Consequently, the noise in this case is essentially non-Gaussian. Only at times $\tau_{12} \ll \bar{v}^{-1}$, which are too short for these most important fluctuators to switch, the decoherence is dominated by the faster fluctuators' contributions, and the Gaussian approximation turns out to be valid.

(ii) When $\bar{v} \gg \gamma_0$ we find

$$\mathcal{K}_{\rm sf}(2\tau_{12}) \approx \begin{cases} 4P_0 T \gamma_0 \bar{v}^2 \tau_{12}^3/3, & \tau_{12} \ll \bar{v}^{-1}, \\ 2P_0 T \gamma_0 \tau_{12}, & \tau_{12} \gg \bar{v}^{-1}. \end{cases} \tag{57}$$

In this case *all* fluctuators are strongly coupled to the qubit. Therefore, the long-time decoherence is essentially non-Gaussian.

We thus conclude that it is the long-time decoherence that is most sensitive to the particular model of the noise. Unfortunately, at long times the signal is usually weak and obscured by noise. One of the possible ways to experimentally identify the non-Gaussian behavior is based on the fact that the typical fluctuator strength, $\bar{v}$, enters the the expressions for the Gaussian and non-Gaussian decay in different ways. In particular, according to the Gaussian approximation, $\mathcal{K}_m(t) \propto \bar{v}^2$ at all times. Contrarily, according to the SF model (equations (56) and (57)), the powers of $\bar{v}$ are different for different times. By fitting to the SF model, this parameter can be extracted, and from this we can infer the flux change corresponding to the flip of a single fluctuator. We have performed such fits to the experimental data of [46]; the details are given in [47], and one example is reproduced in figure 6. As can be seen, it is difficult to determine on the basis of these experiments whether non-Gaussian effects are important, or the Gaussian approximation is sufficient; both the models fit the data equally well. However, *if* we choose to fit the SF model and fit not only to one experimental curve, but also to the whole set of curves for different working points of the qubit, we find that equation (56) for the case $\bar{v} \ll \gamma_0$ provides the better overall fit. The change of flux due to a single fluctuator flip is $\lesssim 10^{-5}\Phi_0$, where Φ_0 is the flux quantum.

5. Microscopic sources of telegraph noise

In this section, we briefly discuss microscopic noise sources that can produce classical telegraph noise.

5.1. Charge noise

The obvious source of RTP charge noise is a charge which jumps between two different locations in space. Where these charges are actually located and what the two states are remains unclear. The first attempt at constructing such a model in relation to qubit decoherence appeared in [22], where electron tunneling between a localized state in the insulator and a metallic gate

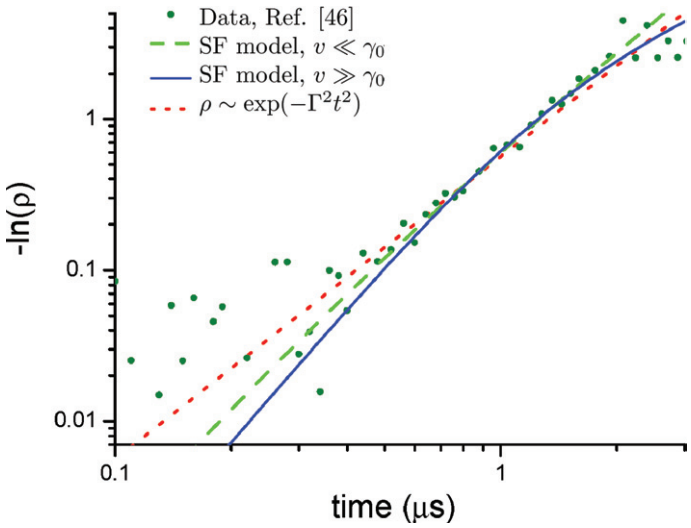

Figure 6. Fit of the experimental data from [46] to the Gaussian model, and to the SF model with $\bar{v} \ll \gamma_0$ (equation (56)) or $\bar{v} \gg \gamma_0$ (equation (57)).

was studied. This model has been further studied in [49, 50]. Later, experimental results [4] indicated a linear dependence of the relaxation rate on the energy splitting of the two qubit states. One also has to take into account that in the experimental setup there is no normal metal in the vicinity of the qubit: all gates and leads should be in the superconducting state at the temperatures of the experiment. These two facts suggest that the model [22] is irrelevant for the decoherence in charge qubits [45] and a model with superconducting electrodes is favored [51]. In this model, the two electrons of a Cooper pair are split and tunnel separately to some localized states in the insulator (see figure 7 for an illustration of this (model III) and other models). A constant density of these localized states gives a linearly increasing density of occupied pairs, in agreement with experiments [4]. This model was criticized [52] because it required an unreasonably high concentration of localized states, and a more elaborate model was proposed. However, it was shown [49, 50] that allowance for quantum effects of hybridization between the electronic states localized at the traps and extended states in the electrodes relaxes the above requirement. At present, it seems that no solid conclusions can be drawn based on the available experiments.

5.2. Noise of critical current

The microscopic mechanism and the source of the fluctuations on the critical current in a Josephson junction are long-standing open problems. These fluctuations were initially attributed to the charges tunneling or hopping between different localized states in the barrier forming glass-like TLSs. However, a more detailed comparison with experiment revealed an important problem—the experimentally observed noise spectrum [53] was proportional to T^2, which is incompatible with the assumption of constant TLS density of states. The interest in the critical current fluctuations was recently renewed because of their importance for superconducting qubits. The new experiments [54] on fluctuations in small Al junctions—similar to those used in several types of qubits [55]—in normal state brought a new puzzle. It turned out that the temperature dependence of the noise power spectrum in the normal state is *linear*, and the noise power is much less than that reported for large superconducting contacts.

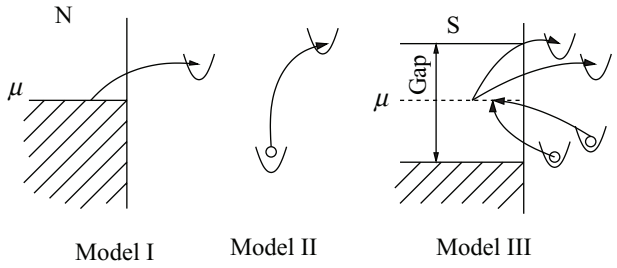

Figure 7. Three possible models for the fluctuating charges: model I, electrons jumping between a localized state and a normal metal, as discussed in [22, 49, 50]; model II, electrons jumping between localized states; and model III, electrons jumping between localized states and a superconductor, as discussed in [51].

A plausible explanation of such behavior is given in [56], where it is suggested that the critical current noise is due to electron trapping in shallow subgap states that might be formed at the superconductor–insulator boundary. This mechanism is similar to that suggested earlier for the charge noise [52].

5.3. Flux noise

Studies of the flux noise in superconducting structures have a long history. As early as in the 1980s it was demonstrated that it is the flux and not the critical current noise that limits the sensitivity of dc SQUIDs [57]. The interest in this problem was recently renewed when it was realized that flux noise can limit the coherence in flux and phase superconducting qubits [46, 58]. Two recent models for fluctuators producing low-frequency noise were suggested. The first one [59] attributes the flux noise to the electron hopping between traps in which their spins have fixed, random orientations. The second one [60] proposes that electrons flip their spins due to interaction with tunneling TLSs and phonons. These models were recently criticized in [61] where it was stated that it is hard to justify the assumptions behind both models. In that paper, a novel mechanism—based on spin diffusion along the surface of a superconductor—was suggested. This model seems to agree with recent experiments [62] on measurements of the $1/f$ noise. It remains to be understood whether the surface spin fluctuations lead to pronounced non-Gaussian behavior in the qubit decoherence.

6. Conclusions

In this review, we have discussed the SF model for qubit dephasing. This model provides a simple, solvable, yet in many situations realistic model of the qubit environment. In particular, we show how to apply the model in situations where the noise shows $1/f$ behavior. The model shows pronounced non-Gaussian behavior, and thus serves as an example of possible deviations from the Gaussian approximation, as well as shedding light on the limitations of the Gaussian approximation.

The main results obtained in studying this model can be summarized as follows.

- A single fluctuator, characterized by the coupling strength v and the switching rate γ, can be classified as weak ($v < \gamma$) or strong ($v > \gamma$). For weak fluctuators the SF model

reproduces the Gaussian result, whereas for strong fluctuators it shows non-Gaussian behavior.

- This non-Gaussian behavior persists even in the limit of long time and for an arbitrary number of independent fluctuators, as long as each fluctuator is strong. This can be understood as a consequence of the δ-functions at the extreme of the phase distribution function.
- In the non-Gaussian case, the time-correlation function of the noise is not sufficient to determine the qubit dephasing and a more detailed model must be specified.
- In the non-Gaussian case, individual fluctuators leave signatures in the measured signal, e. g. plateaus in the echo signal, that can be used to identify the fluctuator parameters.

We should emphasize that a strong fluctuator, giving non-Gaussian effects, does not imply strong decoherence and therefore a bad qubit performance. It indicates only that the coupling is strong relative to the switching rate. However, independently of the performance of the device as a working qubit, i.e. whether it achieves a long dephasing time, we believe that searching for signatures of non-Gaussian behavior can provide valuable information on the nature of the noise source. Given the present uncertain state of understanding of the microscopic sources of noise in most solid-state qubit devices, this seems an important undertaking, and analyzing experiments according to the formulae we have presented can be a useful tool in this process.

Acknowledgments

We are greatful to the Norwegian Research Council for financial support through the STORFORSK and BILAT programs and to NEC-Laboratories America, Argonne National Laboratory, USA, and National Center for Theoretical Sciences of Republic of China, Taiwan for partial financial support and hospitality.

References

[1] Dutta P and Horn P M 1981 *Rev. Mod. Phys.* **53** 497
[2] Weissman M B 1988 *Rev. Mod. Phys.* **60** 537
[3] Zorin A B, Ahlers F J, Niemeyer J, Weimann T, Wolf H, Krupenin V A and Lotkhov S V 1996 *Phys. Rev.* B **53** 13682
[4] Astafiev O, Pashkin Y A, Nakamura Y, Yamamoto T and Tsai J S 2004 *Phys. Rev. Lett.* **93** 267007
[5] Astafiev O, Pashkin Y A, Nakamura Y, Yamamoto T and Tsai J S 2006 *Phys. Rev. Lett.* **96** 137001
[6] Kogan Sh M 1996 *Electronic Noise and Fluctuations in Solids* (Cambridge: Cambridge University Press)
[7] Buckingham M J 1983 *Noise in Electronic Devices and Systems* (New York: Ellis Horwood)
Kirton M J and Uren M J 1989 *Adv. Phys.* **38** 367
[8] Parman C E, Israeloff N E and Kakalios J 1991 *Phys. Rev.* B **44** 8391
Ralls K S, Skocpol W J, Jackel L D, Howard R E, Fetter L A, Epworth R W and Tennent D M 1984 *Phys. Rev. Lett.* **52** 228
Rogers C T and Buhrman R A 1984 *Phys. Rev. Lett.* **53** 1272
Rogers C T and Buhrman R A 1985 *Phys. Rev. Lett.* **55** 859
Duty T, Gunnarsson D, Bladh K and Delsing P 2004 *Phys. Rev.* B **69** 140504(R)
Peters M, Dijkhuis J and Molenkamp L 1999 *J. Appl. Phys.* **86** 1523
Eroms J, van Schaarenburg L, Driessen E, Plantenberg J, Huizinga K, Schouten R, Verbruggen A, Harmans C and Mooij J 2006 *Appl. Phys. Lett.* **89** 122516

[9] Simmonds R W, Lang K M, Hite D A, Nam S, Pappas D P and Martinis J M 2004 *Phys. Rev. Lett.* **93** 077003
Cooper K B, Steffen M, McDermott R, Simmonds R W, Oh S, Hite D A, Pappas D P and Martinis J M 2004 *Phys. Rev. Lett.* **93** 180401
[10] Ithier G, Collin E, Joyez P, Meeson P J, Vion D, Esteve D, Chiarello F, Shnirman A, Makhlin Y, Schriefl J and Schön G 2005 *Phys. Rev.* B **72** 134519
[11] Shnirman A, Schön G, Martin I and Makhlin Y 2005 *Phys. Rev. Lett.* **94** 127002
[12] Klauder R and Anderson P W 1962 *Phys. Rev.* **125** 912
[13] Hu P and Walker L 1997 *Solid State Commun.* **24** 813
Maynard R, Rammal R and Suchail R 1980 *J. Physique Lett.* **41** L291
[14] Black J L and Halperin B I 1977 *Phys. Rev.* B **16** 2879
[15] Moerner W E 1994 *Science* **265** 46
Moerner W E and Orrit M 1999 *Science* **283** 1670
Geva E, Reily P D and Skinner J L 1996 *Acc. Chem. Res.* **29** 579
Barkai E, Jung Y and Silbey R 2001 *Phys. Rev. Lett.* **87** 207403
[16] Ludviksson A, Kree R and Schmid A 1984 *Phys. Rev. Lett.* **52** 950
[17] Kogan S M and Nagaev K E 1984 *Solid State Commun.* **49** 87
[18] Kozub V I 1984 *Sov. Phys.—JETP* **59** 1303
[19] Galperin Y M and Gurevich V L 1991 *Phys. Rev.* B **43** 1290
[20] Galperin Y M, Zou N and Chao K A 1994 *Phys. Rev.* B **49** 13728
[21] Hessling J P and Galperin Y M 1995 *Phys. Rev.* B **52** 5082
[22] Paladino E, Faoro L, Falci G and Fazio R 2002 *Phys. Rev. Lett.* **88** 228304
[23] Paladino E, Faoro L, D'Arrigo A and Falci G 2003 *Physica* E **18** 29
[24] Falci G, Paladino E and Fazio R 2003 *Quantum Phenomena in Mesoscopic Systems* ed B L Altshuler and V Tognetti (Amsterdam: IOS Press) pp 173–98
[25] Galperin Y M, Altshuler B L and Shantsev D V 2004 *Fundamental Problems of Mesoscopic Physics* ed I V Lerner *et al* (Dordrecht: Kluwer) pp 141–65
[26] Falci G, D'Arrigo A, Masteloni A, Paladino E and Fazio R 2004 *Phys. Rev.* A **70** 040101
[27] Falci G, D'Arrigo A, Masteloni A and Paladino E 2005 *Phys. Rev. Lett.* **94** 167002
[28] Galperin Y M, Altshuler B L, Bergli J and Shantsev D V 2006 *Phys. Rev. Lett.* **96** 097009
[29] Martin I and Galperin Y M 2006 *Phys. Rev.* B **73** 180201
[30] Bergli J, Galperin Y M and Altshuler B L 2006 *Phys. Rev.* B **74** 024509
[31] DiVincenzo D P and Loss D 2005 *Phys. Rev.* B **71** 035318
Lutchyn R M, Cywiński L, Nave C P and Das Sarma S 2008 *Phys. Rev.* B **78** 024508
Coish W A, Fischer J and Loss D 2008 *Phys. Rev.* B **77** 125329
[32] Galperin Y M, Shantsev D V, Bergli J and Altshuler B L 2005 *Europhys. Lett.* **71** 21
[33] Paladino E, Sassetti M, Falci G and Weiss U 2008 *Phys. Rev.* B **77** 041303(R)
[34] Charles P S 1978 *Principles of Magnetic Resonance* (*Springer Series in Solid-State Sciences* vol 1) ed M Cardona and H J Queisser (Berlin: Springer)
[35] Astafiev O, Pashkin Y A, Nakamura Y, Yamamoto T and Tsai J S 2004 *Phys. Rev.* B **69** 180507(R)
[36] Mims W B 1972 *Electron Paramagnetic Resonance* ed S Geschwind (New York: Plenum) pp 263–351
[37] Itakura T and Tokura Y 2003 *Phys. Rev.* B **67** 195320
[38] Anderson P W, Halperin B I and Varma C M 1972 *Phil. Mag.* **25** 1
Phillips W A 1972 *J. Low Temp. Phys.* **7** 351
[39] Jäckle J 1972 *Z. Phys.* **257** 212
[40] Black J L and Gyorffy B L 1978 *Phys. Rev. Lett.* **41** 1595
Black J L 1981 *Glassy Metals, Ionic Structure, Electronic Transport and Crystallization* (New York: Springer) pp 167–73
[41] Halperin B I 1976 *Ann. NY Acad. Sci.* **279** 173
Black J L 1978 *Phys. Rev.* B **17** 2740

[42] Laikhtman B D 1985 *Phys. Rev.* B **31** 490
[43] Chandrasekhar S 1943 *Rev. Mod. Phys.* **15** 1
[44] Lundin N I and Galperin Y M 2001 *Phys. Rev.* B **63** 094505
[45] Nakamura Y, Pashkin Yu A, Yamamoto T and Tsai J S 2002 *Phys. Rev. Lett.* **88** 047901
[46] Yoshihara F, Harrabi K, Niskainen A O, Nakamura Y and Tsai J S 2006 *Phys. Rev. Lett.* **97** 167001
[47] Galperin Y M, Altshuler B L, Bergli J, Shantsev D and Vinokur V 2007 *Phys. Rev.* B **76** 064531
[48] Harris R *et al* 2008 *Phys. Rev. Lett.* **101** 117003
[49] Grishin A, Yurkevich I V and Lerner I V 2005 *Phys. Rev.* B **72** 060509
[50] Abel B and Marquardt F 2008 arXiv:0805.0962
[51] Faoro L, Bergli J, Altshuler B L and Galperin Yu M 2005 *Phys. Rev. Lett.* **95** 046805
[52] Faoro L and Ioffe L B 2006 *Phys. Rev. Lett.* **96** 047001
[53] Wellstood F C, Urbina C and Clarke J 2004 *Appl. Phys. Lett.* **85** 5296
van Harlingen D J, Robertson T L, Plourde B L T, Reichardt P A, Crane T A and Clarke J 2004 *Phys. Rev.* B **70** 064517
[54] Eroms J, van Schaarenburg L C, Driessen E F C, Plantenberg J H, Huizinga C M, Schouten R N, Verbruggen A H, Harmans C J P M and Mooij J E 2006 *Appl. Phys. Lett.* **89** 122516
[55] Chiorescu I, Nakamura Y, Harmans C J P M and Mooij J E 2003 *Science* **299** 1869
Martinis J M, Nam S, Aumentado J and Urbina C 2002 *Phys. Rev. Lett.* **89** 117901
Vion D, Aassime A, Cottet A, Joyez P, Pothier H, Urbina C, Esteve D and Devoret M H 2002 *Science* **96** 886
[56] Faoro L and Ioffe L B 2007 *Phys. Rev.* B **75** 132505
[57] Koch R H, Clarke J, Goubau W M, Martinis J M, Pegrum C M and van Harlingen D J 1983 *J. Low Temp. Phys.* **51** 207
Wellstood F C, Urbina C and Clarke J 1987 *Appl. Phys. Lett.* **50** 772
[58] Martinis J M, Nam S, Aumentado J and Lang K M 2003 *Phys. Rev.* B **67** 094510
[59] Koch R H, DiVincenzo D P and Clarke J 2007 *Phys. Rev. Lett.* **98** 267003
[60] de Sousa R 2007 *Phys. Rev.* B **76** 245306
[61] Faoro L and Ioffe L B 2008 *Phys. Rev. Lett.* **100** 227005
[62] Bialczak R C, McDermot R, Ansmann M, Hofheinz H, Katz N, Lucero E, Neeley M, O'Connel A D, Wang H, Cleland A N and Martinis J M 2007 *Phys. Rev. Lett.* **99** 187006
Sendelbach S, Hover D, Kittel A, Mück M, Martinis J M and McDermott R 2008 *Phys. Rev. Lett.* **100** 227006